THE JOURNAL OF PHYSICAL CHEMISTRY A

 VOLUME 105, NUMBER 40, OCTOBER 11, 2001

ARTICLES

A Comparison of Simulated and Experimental Voltammograms Obtained for the $[Fe(CN)_6]^{3-/4-}$ Couple in the Absence of Added Supporting Electrolyte at a Rotating Disk Electrode

N. P. C. Stevens, M. B. Rooney, A. M. Bond,* and S. W. Feldberg†

School of Chemistry, Monash University, Clayton, Victoria 3800, Australia

Received: January 31, 2001; In Final Form: June 9, 2001

The voltammetric behavior of the $[Fe(CN)_6]^{3-/4-}$ couple at a glassy carbon rotating macrodisk electrode without added supporting electrolyte is shown to be in close to ideal agreement with the theory presented over a wide range of electrode rotation and scan rates when the concentration of electroactive species used is 50 mM. The influences of migration, uncompensated resistance, heterogeneous charge-transfer kinetics, and inhomogeneous diffusion are shown to be well modeled by a finite difference simulation scheme that affords excellent agreement between experiment and theory. The use of the rotating disk electrode, even when only moderate rotation rates are employed, is shown to eliminate the problem with natural convection that exists when using stationary electrodes (macro- or microdisk) and that is enhanced in the absence of added supporting electrolyte. Consequently, it has been concluded that the rotating disk electrode method represents an almost ideal technique for conducting studies without added supporting electrolyte.

Introduction

The early history of voltammetry, mainly using polarography at a dropping mercury electrode, contains examples of studies of systems with little or no added supporting electrolyte (ASE). Problems caused by diffuse double layers were examined[1] and for the most part remedied by the addition of a large excess of ASE—an approach commonly used in modern forms of voltammetry. However, there has been a recent renewed interest in the electrochemical behavior of systems utilizing no ASE[2−8] facilitated by the use of microelectrodes. The motivations for and against using solutions containing ASE have been well discussed in the literature.[9,10] Major advantages of using ASE are that increased solution conductivity decreases the IR_u drop (I = current, R_u = uncompensated resistance) and that migration of the species under study is diminished. The main disadvantage of requiring ASE is the possibility of influencing the physical characteristics of the analyte and solvent, so that data obtained by other physiochemical techniques may not be directly comparable.

The new generation of studies of partially supported and unsupported electrochemistry have focused almost exclusively on microelectrodes[2−8] of disk, hemispherical,[11−13] cylindrical, or band[14] geometries. The implication of the emphasis on steady-state or near-steady-state conditions is that macroelectrode techniques that are widely used in studies with ASE have been assumed to be unsuitable for use without ASE. However, it can be noted that while experimental data are scarce, the response to a potential step at a macroelectrode[15] has been considered theoretically, assuming that if a sufficient overpotential is applied, then the IR_u drop is of no consequence. Likewise, the

* To whom correspondence should be addressed. Phone: +61 3 9905 4507. Fax: +61 3 9905 4597. E-mail: Alan.Bond@sci.monash.edu.au.

† On leave from the Department of Applied Science, Building 815, Brookhaven National Laboratory, Upton, NY 11973-5000.

10.1021/jp0103878 CCC: $20.00
Published on Web 09/20/2001

steady-state limiting current response at a rotating disk electrode (RDE) is unaffected in magnitude by the IR_u drop, and has been treated analytically.[16]

A more subtle problem that attends transient voltammetry at macroelectrodes[17] and microelectrodes,[18] supported or not, is that of natural convection.[19] Arising from density gradients engendered by variations in temperature and solution composition, the effects of natural convection augment diffusional and migrational transport. Although temperature variations can easily be eliminated, alteration of the solution density by the interconversion of species at the electrode cannot, but it can be reduced by decreasing the analyte concentrations. However, with dilute analyte concentrations in the absence of ASE, effects arising from a very diffuse double layer can be problematical.[20]

In line with the above discussion, a major motivation for the present study was to develop methods that eliminate or minimize distortions of the electrochemical responses caused by density gradients which are electrochemically introduced in the depletion region adjacent to the electrode. Clearly, the use of the RDE should represent a useful approach to addressing this problem, although no complete theoretical description of this technique is available. It is simple to demonstrate that a consequence of operating with no ASE is that the density variations within the depletion region are generally exacerbated; furthermore, it is obvious that these density variations will scale with the concentration of the electroactive species. To amplify the density effect, we have chosen to work with high concentrations (50 mM) of potassium ferricyanide/ferrocyanide, a stable, convenient, inexpensive, and chemically reversible system. Serendipitously, the high concentrations minimize Frumkin effects, which are believed to be an important cause of problems reported at low ferri/ferrocyanide concentrations.[19−22] Of course, the use of high concentrations will often compromise the goals of working with no ASE. However, in previous work[19] we demonstrated that cyclic voltammetry of low concentrations (~1 mM) of high molecular mass electroactive species can exhibit density-induced distortions. We will show that carrying out the electrochemistry at an RDE effectively eliminates the effects of natural convection and suggests the hypothesis that voltammetry at the RDE may be the preferred technique for voltammetric studies without ASE. Simulations of the RDE system with no ASE accurately describe the experimental responses.

Experimental Section

Reagents. Potassium ferricyanide ($K_3[Fe(CN)_6]$), potassium ferrocyanide ($K_4[Fe(CN)_6]$), and potassium chloride (KCl) were Analar grade products, used as received. For those experiments in which supporting electrolyte was present, KCl was added to give a 1 M concentration. All solutions were prepared with water from a MilliQ-MilliRho purification system (18 MΩ cm), and were found to have a typical pH value of 6.5.

Electrochemistry. Voltammetry was performed using a Bioanalytical Systems (BAS) model 100B electrochemistry system equipped with a peripheral assembly for rotating disk measurements (Bioanalytical Systems, West Lafayette, IN). All experiments were performed in a three-electrode cell. The auxiliary electrode was a Pt wire, the end of which was approximately 2 cm from the working electrode. Although a conventional reference electrode system can result in leakage of ions that can have a significant effect on electrochemistry of low analyte concentrations in the absence of deliberately added ASE, the use of a Ag/AgCl reference electrode (saturated KCl) was found to have a negligible effect on electrochemical measurements of high concentrations (≥50 mM) of $K_3Fe(CN)_6$ and $K_4Fe(CN)_6$ in the absence of ASE. For this reason, the Ag/AgCl reference electrode was used for all electrochemical measurements at these high analyte concentrations (50 mM). The distance between the reference and working electrodes was approximately 1 cm. The working electrode was a glassy carbon (GC) macroelectrode (diameter 2.92 mm) which prior to each voltammetric experiment was manually polished with an aqueous slurry of 0.1 or 0.05 μm alumina particles (Bioanalytical Systems) on a Microcloth polishing cloth (Buehler, Lake Bluff, IL) and then rinsed thoroughly with water.

Various combinations of scan rates and rotation rates were employed with each set of conditions, as specified in the figure captions. Typically, voltammetric studies at each scan/rotation rate combination were conducted in the same solution of $K_4[Fe(CN)_6]$ or $K_3[Fe(CN)_6]$. To minimize the interference of oxygen, the solutions were purged with high-purity nitrogen prior to working electrode placement and subsequent voltammetry. All experiments were performed with the cell at room temperature (293 K).

The resistances measured experimentally for solutions without ASE used the time decay method provided with the BAS electrochemical analyzer.[23,24]

Theory

Analytical solutions exist for the limiting current for completely unsupported voltammetry when only three ions are present[9,12,13,15] (reactant, product, and counterion). These theoretical studies proceed from the assumption of electroneutrality and homogeneous diffusion coefficients for the three species present, under which conditions there is only 1 degree of freedom for the solution composition, which may be conveniently expressed in terms of the ionic strength. In the present paper, the problems approached involve only three ionic species for the unsupported work, and four for solutions containing ASE. The simulation package developed to model such systems can include an arbitrary number of electroactive and electroinactive species. Thus, to avoid duplication of material in future publications, the general scheme is presented for an arbitrary number of species, rather than just those parts necessary to model the three or four species problems.

Applicable Systems. The scheme presented accommodates any number j of species s_j of which any number up to $j - 1$ may form sequential couples of the form $s_1 + ne^- \rightarrow s_2 + ne^- \rightarrow s_3$ or any number of separate couples, $s_1 + ne^- \rightarrow s_2$, $s_3 + ne^- \rightarrow s_4$, or any combination thereof, with species j being a counterion to an ionic species present. Alternatively, if only neutral forms of the electroactive species are initially present, two supporting ionic species of opposite sign must be present. Any number of additional electroinactive species may also be present. The electrode is assumed to be large and planar, and may be stationary, or take the form of a rotating disk. The scheme presented calculates the IR_u drop between the reference electrode (three-electrode case) or counter electrode (two-electrode case) and the working electrode on the basis of a calculated distance between the two.

Catalog of Physical Laws. The flux of a species j through the solution is given as f_j by the Nernst−Planck relationship, given by eq 1, where f_j is the flux density of species j (mol

$$f_j = -D_j \frac{dc_j}{dx} - D_j c_j z_j \frac{F}{RT} \frac{d\phi}{dx} \qquad (1)$$

cm^{-2} s^{-1}), c_j is the concentration of species j, z_j is the charge number of species j, $-d\phi/dx$ is the electric field (V cm^{-1}), which

is the negative gradient of the electric potential, and D_j is the diffusion coefficient of species j ($cm^2\ s^{-1}$).

The flux with respect to the solution (as opposed to the flux through a static plane) is assumed not to be coupled to motion of the solution itself, the velocity of which may be given by the Levich equation for the RDE (eq 2) or a modification thereof

$$u = -0.510\omega^{3/2}\nu^{-1/2}x^2 \tag{2}$$

(eq 31), or may be zero for a stationary macroplanar electrode. In eq 2, u is the solution velocity in the direction normal to the electrode ($cm\ s^{-1}$), ω is the angular velocity ($rad\ s^{-1}$), ν is the kinematic viscosity ($cm^2\ s^{-1}$), and x is the distance from the electrode (cm).

If the fluxes of solute species through the solvent and the solution velocity are assumed separable, the rate of concentration change with time may therefore be expressed as

$$\frac{dc_j}{dt} = -\frac{df_j}{dx} - u\frac{dc_j}{dx} \tag{3}$$

Electroneutrality is assumed at all points of interest, giving eqs 4 and 5.

$$\sum_{j=1}^{n} c_j z_j = 0 \tag{4}$$

$$\sum_{j=1}^{n} (dc_j/dx) z_j = 0 \tag{5}$$

This assumption is entirely valid for the bulk solution and is only called into question in regions near enough to the electrode to lie within the diffuse double layer predicted by Gouy−Chapman theory. In the present case, the ionic strength is sufficient to allow this region to become negligibly small.

The interfacial kinetics at the surface of the electrode are assumed to be governed by the Butler−Volmer[17] relationship (eq 6). In eq 6, species j and $j + 1$ are a redox couple with

$$f_j^0 = -k_{f,j}c_j^0 + k_{b,j}c_{j+1}^0 \tag{6}$$

forward and reverse rate constants k_f and k_b ($cm\ s^{-1}$) and the 0 superscript denotes a value at the electrode surface. Depending on whether the redox process is an oxidation or a reduction, the rate constants of the forward and reverse reactions may be identified as k_{ox} and k_{red} or as k_{red} and k_{ox}, respectively, given by eq 7,

$$k_{ox} = k^{0\prime}\exp\left(\frac{(1-\alpha)F(E_{eff} - E^{0\prime})}{RT}\right)$$
$$k_{red} = k^{0\prime}\exp\left(\frac{-\alpha F(E_{eff} - E^{0\prime})}{RT}\right) \tag{7}$$

where $k^{0\prime}$ is the formal heterogeneous electron-transfer rate constant, E_{eff} is the potential across the electrode double layer, and $E^{0\prime}$ is the formal reversible potential of the redox couple.

Derivation of the Simulation Model. The grid used to discretize the concentration and potential distributions is as shown in Figure 1, along with a summary of the variables defined at the nodes, or at the midpoints between the nodes.

The grid used is expanding, with the first node on the electrode surface, and subsequent nodes numbered as shown in Figure 1 located $\beta^{i-1}\Delta x$ cm from the electrode surface. The limit of the simulated region is given by finding the minimum

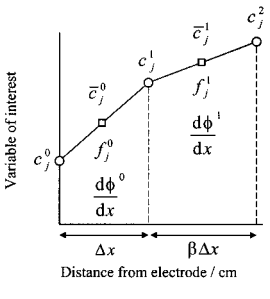

c_j^i Concentration of species j at node i.

$\bar{c}_j^i$ Concentration of species j at midpoint between nodes i and i+1, found as the mean of the values at nodes i and i+1.

f_j^i Flux density at midpoint between nodes i and i+1.

$\frac{d\phi}{dx}^i$ Potential gradient at midpoint between nodes i and i+1.

Figure 1. Grid used for the finite difference simulation.

extent of the diffusion layer predicted for the hydrodynamic steady state, x_{RDE}, eq 8, or the transient case after the total duration of the experiment, x_{trans}, eq 9.

$$x_{RDE} = 4D^{1/3}\nu^{1/6}\omega^{-1/2} \tag{8}$$

$$x_{trans} = 6D^{1/2}\pi^{1/2}t_{max}^{1/2} \tag{9}$$

The number of nodes used and the value of Δx may be set by the user, although 40−100 nodes and Δx values of 10^{-3} cm were found to give more than sufficient grid refinement for the problem of interest in this paper.

To find the flux of charge through a plane carried by a species, eq 1 is multiplied by z_j. If this flux is divided by the diffusion coefficient, and summation over all species considered, then

$$\sum_{j=1}^{n}\frac{f_j z_j}{D_j} = -\sum_{j=1}^{n}\frac{dc_j}{dx}z_j - \frac{F}{RT}\frac{d\phi}{dx}\sum_{j=1}^{n}c_j z_j^2 \tag{10}$$

However, assuming electroneutrality, the second term is equal to zero, so the potential gradient may be found as

$$\frac{F}{RT}\frac{d\phi}{dx} = \frac{-\sum_{j=1}^{n}(f_j z_j/D_j)}{\sum_{j=1}^{n}c_j z_j^2} \tag{11}$$

The concentration gradient for the species required for solution of the equation is approximated by

$$\frac{dc_j}{dx} = \frac{c_j^{i+1} - c_j^i}{\Delta x} \tag{12}$$

Substitution of eq 12 into eq 1 gives

$$f_j = -D_j\frac{c_j^{i+1} - c_j^i}{\Delta x} - D_j\bar{c}_j^i z_j\frac{F}{RT}\frac{d\phi^i}{dx} \tag{13}$$

where c_j^i is the concentration of species j at node i, $\bar{c}_j^i$ is the concentration at the midpoint between nodes i and $i + 1$, found as the average of the two nodal concentrations, and $d\phi^i/dx$ is the gradient of the potential over the same region. Multiplying this equation by $\Delta t/\Delta x$ gives

$$\frac{\Delta t}{\Delta x}f_j = -D_j\Delta t\frac{c_j^{i+1} - c_j^i}{\Delta x^2} - \frac{\Delta t}{\Delta x}D_j\bar{c}_j^i z_j\frac{F}{RT}\frac{d\phi^i}{dx} \tag{14}$$

Defining $\Delta t = 0.4\Delta x^2/D_{max}$, where D_{max} is the largest diffusion coefficient of any species present, ensures that the explicit time

stepping scheme used will be stable.[25] Setting $D_j^* = 0.4D_j/D_{max}$, which is dimensionless, $f_j^* = (\Delta t/\Delta x)f_j$, which has units of concentration, and $d\phi^{i*}/dx = \Delta x(F/RT)(d\phi^i/dx)$, which is dimensionless, gives

$$f_j^* = -D_j^*(c_j^{i+1} - c_j^i) - D_j^*\bar{c}_j^i z_j \frac{d\phi^{i*}}{dx} \tag{15}$$

where the asterisk denotes the normalized form of each variable. Multiplying eq 6 by $\Delta t/\Delta x$ and setting the dimensionless rate constant $k_{f,j}^* = (\Delta t/\Delta x)k_{f,j}$ gives

$$f_j^{0*} = -k_{f,j}^* c_j^0 + k_{b,j}^* c_{j+1}^0 \tag{16}$$

If $\bar{c}_j^0$ is approximated by c_j^0 eq 15 may be rearranged to find the concentration of species j at the electrode surface:

$$c_j^0 = \left(\frac{f_j^{0*}}{D_j^*} + c_j^1\right)\left(1 - z_j\frac{d\phi^{0*}}{dx}\right)^{-1} \tag{17}$$

Defining $\chi_j^0 = [1 - z_j(d\phi^{0*}/dx)]^{-1}$ and substituting eq 17 into eq 16 gives

$$f_j^{0*} = -k_{f,j}^*\left(\frac{f_j^{0*}}{D_j^*} + c_j^1\right)\chi_j^0 + k_{b,j}\left(\frac{f_{j+1}^{0*}}{D_{j+1}^*} + c_{j+1}^1\right)\chi_{j+1}^0 \tag{18}$$

This may be rearranged to find the fluxes of species j and $j + 1$:

$$\left(1 + \frac{k_{f,j}^*\chi_j^0}{D_j^*}\right)f_j^{0*} - \frac{k_{b,j}^*\chi_{j+1}^0}{D_{j+1}^*}f_{j+1}^{0*} = -k_{f,j}^*\chi_j^0 c_j^1 + k_{b,j}^*\chi_{j+1}^0 c_{j+1}^1 \tag{19}$$

which may be stated as

$$a_j f_j^{0*} + b_j f_{j+1}^{0*} = -k_{f,j}^*\chi_j^0 c_j^1 + k_{b,j}^*\chi_{j+1}^0 c_{j+1}^1 \tag{20}$$

The principle of conservation of material requires that the sum of the fluxes of all reactants and products at the electrode surface must be zero (for simple electron transfers):

$$\sum_{j=1}^{n} f_j^{0*} = 0 \tag{21}$$

By simultaneously solving eqs 20 and 21 for all couples, the fluxes at the electrode may be found. The system of equations is expressed in matrix form for one couple, $s_1 + ne^- \rightarrow s_2$, as

$$\begin{bmatrix} a_1 & b_1 \\ 1 & 1 \end{bmatrix}\begin{bmatrix} f_1^{0*} \\ f_2^{0*} \end{bmatrix} = \begin{bmatrix} -k_{f,1}^* E_1^0 c_1^1 + k_{b,1}^* E_2^0 c_2^1 \\ 0 \end{bmatrix} \tag{22}$$

or for three sequential couples, $s_1 + ne^- \rightarrow s_2 + ne^- \rightarrow s_3 + ne^- \rightarrow s_4$, as

$$\begin{bmatrix} a_1 & b_1 & & \\ & a_2 & b_2 & \\ & & a_3 & b_3 \\ 1 & 1 & 1 & 1 \end{bmatrix}\begin{bmatrix} f_1^{0*} \\ f_2^{0*} \\ f_3^{0*} \\ f_4^{0*} \end{bmatrix} = \begin{bmatrix} -k_{f,1}^* E_1^0 c_1^1 + k_{b,1}^* E_2^0 c_2^1 \\ -k_{f,2}^* E_2^0 c_2^1 + k_{b,2}^* E_3^0 c_3^1 \\ -k_{f,3}^* E_3^0 c_3^1 + k_{b,3}^* E_4^0 c_4^1 \\ 0 \end{bmatrix} \tag{23}$$

or for two separate couples, $s_1 + ne^- \rightarrow s_2$ and $s_3 + ne^- \rightarrow s_4$, as

$$\begin{bmatrix} a_1 & b_1 & & \\ 1 & 1 & & \\ & & a_3 & b_3 \\ & & 1 & 1 \end{bmatrix}\begin{bmatrix} f_1^{0*} \\ f_2^{0*} \\ f_3^{0*} \\ f_4^{0*} \end{bmatrix} = \begin{bmatrix} -k_{f,1}^* E_1^0 c_1^1 + k_{b,1}^* E_2^0 c_2^1 \\ 0 \\ -k_{f,3}^* E_3^0 c_3^1 + k_{b,3}^* E_4^0 c_4^1 \\ 0 \end{bmatrix} \tag{24}$$

Once the fluxes at the surface are known, the surface concentrations may be calculated as in eq 17, and the electric field term at the surface may be calculated as in eq 11. As the electric field term is a factor on the right-hand side of eq 20, an iterative scheme is employed: (1) Assume a trial value for $d\phi/dx^{0*}$. (2) Solve the appropriate matrix equation of the form of eqs 22−24 to determine the surface flux of each electroactive species. (3) Solve eq 11 to find a resulting value for $d\phi/dx^{0*}$. (4) Determine a new trial value for $d\phi/dx^{0*}$ for the next iteration using the bisection search algorithm taking account of previous trials and results.

This calculation must be reiterated until the change over an iteration as a fraction of the trial value becomes acceptably small, e.g., less than 10^{-12}.

The total current density arising from all interfacial processes may be found as

$$i_{total} = F\sum_{j}^{n} f_j z_j \tag{25}$$

Once the current density at the electrode surface is known, the fluxes of each component at all other planes parallel to the surface may be calculated. This proceeds first from eq 1, and second from the knowledge that the current flowing through every equipotential surface must be equal for electroneutrality to be preserved—the two requirements indicating that eq 25 must hold at all points. The fluxes at each plane i above the surface can therefore be found by the solution of a matrix equation of the form

$$\begin{bmatrix} 1 & & & a_1 \\ & 1 & & a_2 \\ & & 1 & a_3 \\ z_1 & z_2 & z_3 & 0 \end{bmatrix}\begin{bmatrix} f_1^{i*} \\ f_2^{i*} \\ f_3^{i*} \\ d\phi^{i*}/dx \end{bmatrix} = \begin{bmatrix} D_1^*(c_1^{i+1} - c_1^i) \\ D_2^*(c_2^{i+1} - c_2^i) \\ D_3^*(c_3^{i+1} - c_3^i) \\ i_{total}/F \end{bmatrix} \tag{26}$$

where f_j^{i*} indicates the normalized flux of species j between planes i and $I + 1$, and $a_j = -D_j^* z_j \bar{c}_j^i$. Note that as the fluxes are considered to be defined at the midpoint between two planes, it is the concentrations at these midpoints that appear in the above equation.

As eq 26 also recovers the normalized potential gradient at the midpoint between every node, the potential variation from the working electrode to the auxiliary electrode may be recovered. The potential drop is usually defined as

$$E_{eff} = E_{app} - IR_u \tag{27}$$

where E_{app} is a linear function of both time and scan rate. But if the potential gradient is known over the simulated region, then eq 27 may be restated as

$$E_{eff} = E_{app} + \int_0^{x_{AE}} d\phi/dx \tag{28}$$

where E_{eff} is the potential across the double layer at the working electrode, x_{AE} is the distance of the auxiliary electrode from the working electrode, and E_{app} is the potential difference applied between the working and reference electrodes. As E_{eff} also

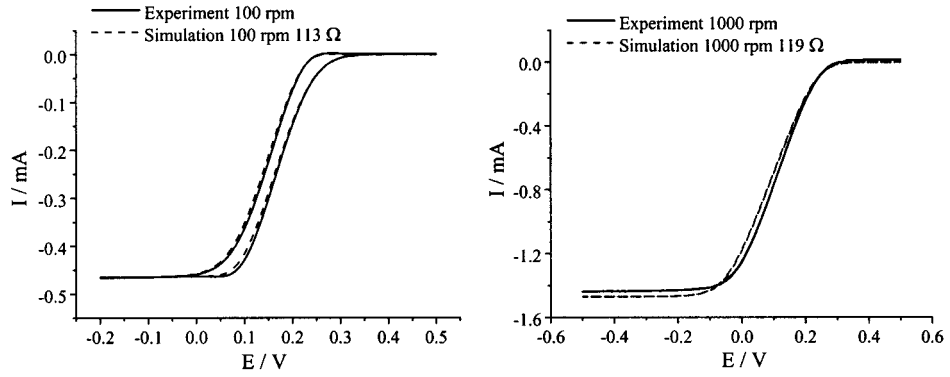

Figure 2. Simulated and experimental cyclic voltammograms for the reduction of 50 mM ferricyanide without ASE at a glassy carbon RDE using a scan rate of 20mV s^{-1} and the indicated rotation rates.

appears in eq 7 the simulation must adopt an iterative procedure, where within each time step a value of E_{eff} is sought at which eqs 7 and 28 are both satisfied. The routine is as follows: (1) Assume a trial value of E_{eff}.

(2) Iteratively solve the equations for the surface flux as previously described.

(3) Solve eq 26 for all points in the simulated region.

(4) Find the potential drop between the working electrode and the reference electrode, and determine a resulting value of E_{eff}.

(5) Determine an improved trial value for E_{eff} using the bisection search method.

This iterative process is continued until the trial and result values differ from one another by an amount which is sufficiently small when expressed as a fraction of the trial value, 10^{-6} being typical. When the potential drop in step 4 is determined, the two possible cases are that the auxiliary electrode lies beyond the edge of the simulated region, or inside it. In the first case the potential gradient in the region outside the simulation may be assumed to be identical to that over the furthest simulated region from the working electrode, as at the extreme away from the electrode the solution composition should remain identical to that of the bulk. If the auxiliary electrode is within the simulated region, the potential drop is integrated over the region only up to the electrode location. In either case, a simple trapezoidal summation is taken. The effects of uncompensated resistance on voltammetry have been extensively studied,[4,8,10,26−29] and computer modeling is often employed.

Once a satisfactory value for E_{eff} is found, the current can be calculated from all the current density found in eq 25, and the concentrations updated. Expressing eq 3 in discretized form gives

$$\frac{dc_j^i}{dt} = \frac{f_j^{i-1} - f_j^i}{\beta^{i-1}\Delta x} - u^i\left(\frac{c_j^{i-1} - c_j^{i+1}}{(\beta^{i-1} + \beta^i)\Delta x}\right) \tag{29}$$

From eq 29 the rate of change in all the concentrations over the time step may be found. The new concentration profiles at the end of the time step, at time $t + \Delta t$, are then found by applying eq 30, where $\beta^{i-1}\Delta x$ is the separation between nodes

$$c_j^{i,t+\Delta t} = c_j^{i,t} + f_j^{i-1*} - f_j^{i*} - (\Delta t)u^i\left(\frac{c_j^{i-1} - c_j^{i+1}}{(\beta^{i-1} + \beta^i)\Delta x}\right) \tag{30}$$

in the expanding grid shown in Figure 1. The solution velocity profile is commonly defined by the Levich[30] approximation, eq 2. Equation 2 overestimates the true velocity profile, but is still accurate at high Schmidt numbers, $Sc = \nu/D$, when the diffusion layer is very thin and lies entirely within the region where this velocity approximation is most accurate. More accurate treatments of the velocity profile have been offered, with one of the most accurate being that used by Feldberg.[31] The calculation of this convection profile may be simplified by the adoption of a dimensionless x coordinate, $\zeta = \omega^{1/2}\nu^{-1/2}x$. The velocity profile is then given by eq 31, which was the form employed in the present study.

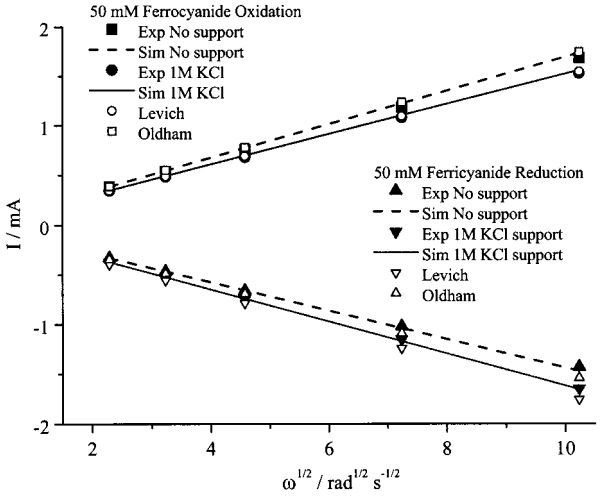

Figure 3. Theoretically and experimentally determined limiting currents obtained at a glassy carbon RDE as a function of rotation rate for oxidation of 50 mM $K_4[Fe(CN)_6]$ or reduction of 50 mM $K_3[Fe(CN)_6]$ at a scan rate of 20 mV s^{-1}, with and without 1 M KCl.

$$u_x = -\omega^{1/2}\nu^{1/2}\left(\frac{0.88447S}{0.88447 + S}\right)$$

$$S = 0.51023\zeta^2 - 0.32381\zeta^3 + 0.34474\zeta^4 - 0.25972\zeta^5 + 0.16214\zeta^6 - 0.07143\zeta^7 + 0.019911\zeta^8 - 0.0030405\zeta^9 + 0.00019181\zeta^{10} \tag{31}$$

For each subsequent time step, the value of E_{app} is updated if necessary, and the steps repeated.

Ionic Enrichment/Depletion. The conductivity of the solution is found as a sum over all the ionic components of the solution:

$$\kappa = F\sum_i |z_i| u_i c_i \tag{32}$$

where κ is the conductivity (Ω^{-1} cm^{-1}) and u_i is the ionic

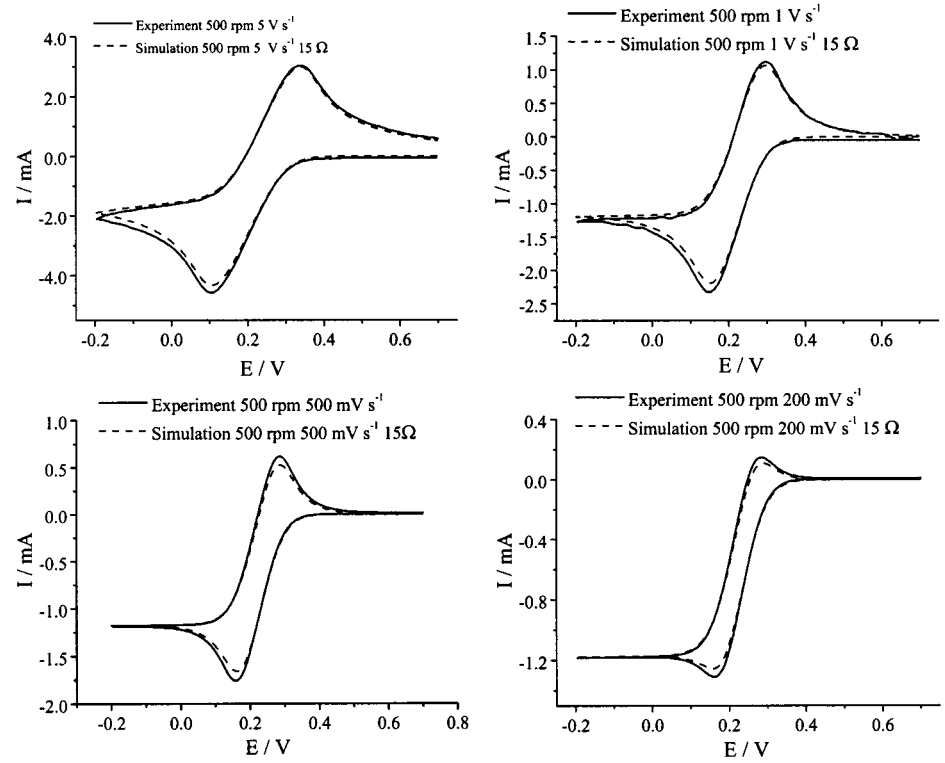

Figure 4. Comparison of simulated and experimental voltammograms for reduction of 50 mM ferricyanide in the presence of 1 M KCl ASE at a glassy carbon RDE using a rotation rate of 500 rpm and the indicated scan rates and R_u values.

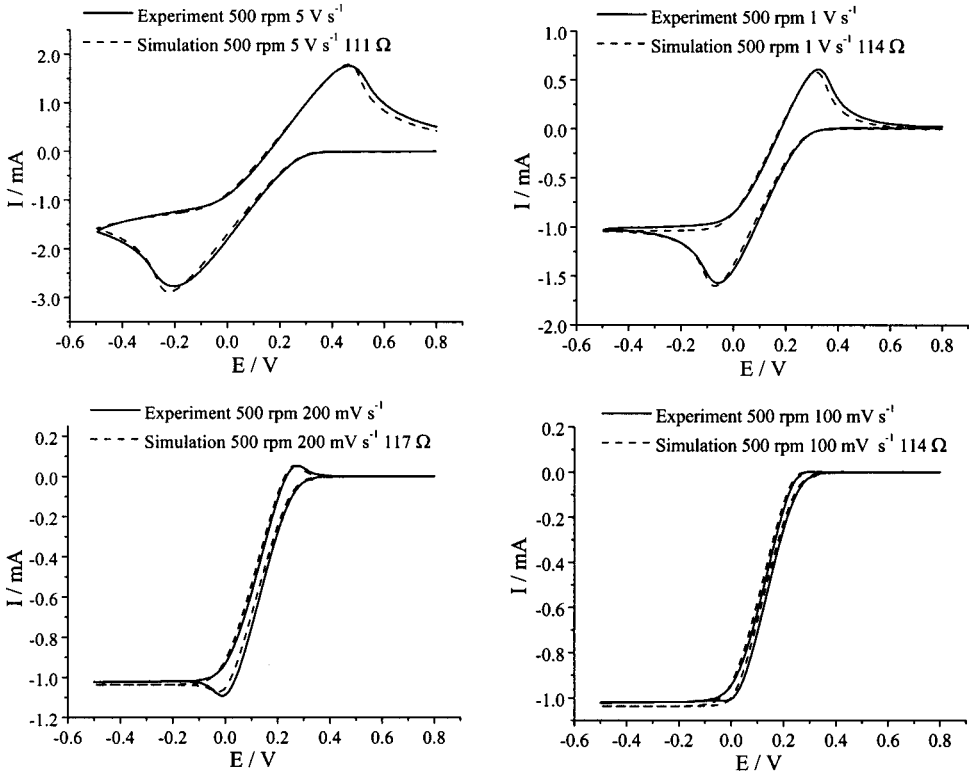

Figure 5. Comparison of simulated and experimental voltammograms for reduction of 50 mM ferricyanide with no ASE at a glassy carbon RDE using a rotation rate of 500 rpm and the indicated scan rates and R_u values.

mobility of species i and may be related to the diffusion coefficient D_i by $u_i = |z_i|(F/RT)D_i$.

It is clear that, at any potential where an electrode reaction proceeds, the conductivity in the vicinity of the electrode will be increased if the magnitudes of the charges of the products of the reactions exceed those of the reactants, and vice versa. This ionic depletion or enrichment[32−34] of the solution in the diffusion layer has been found to be most problematic when neutral redox species are involved, but this situation does not apply in the present investigation.

Since the simulation described above relates the electric field at every point to the local fluxes and concentrations via eq 11,

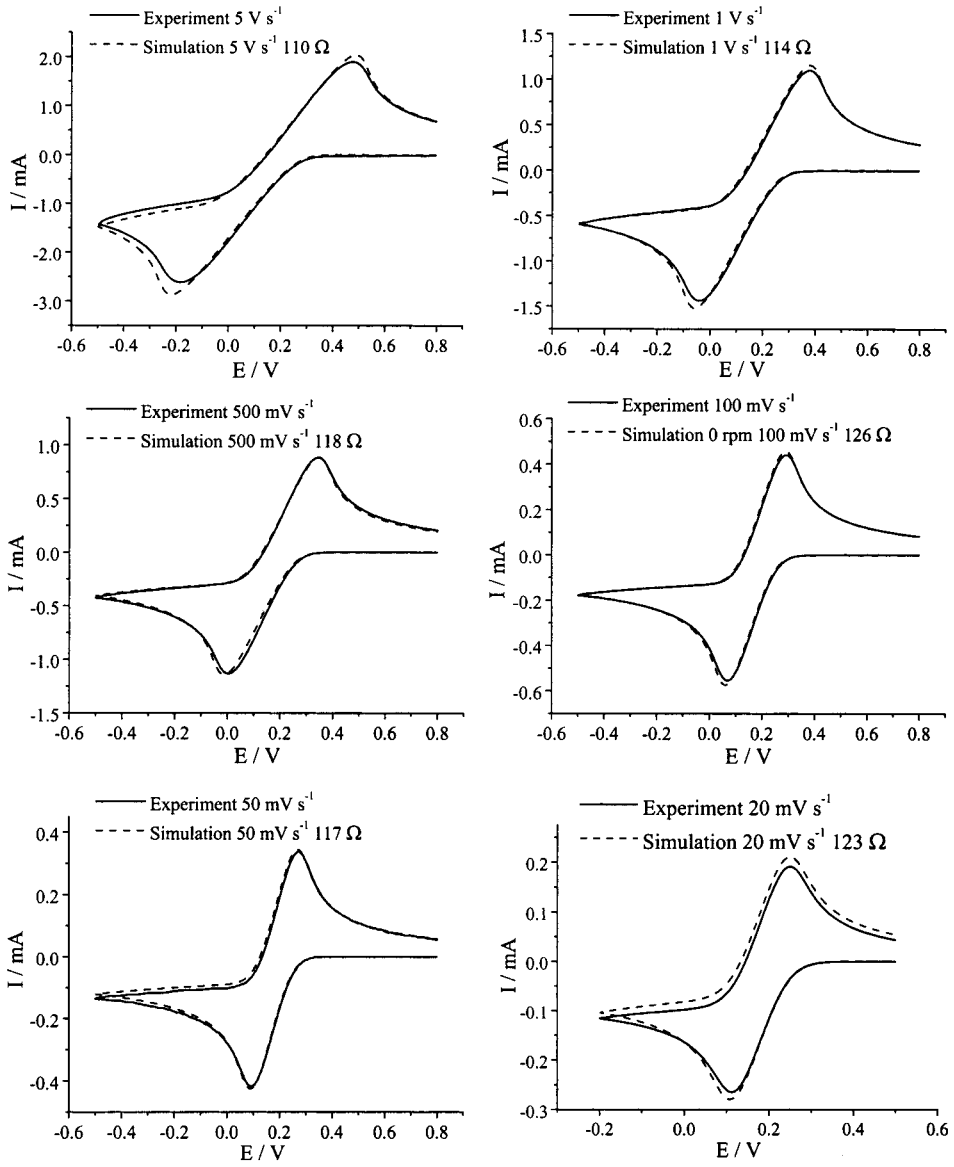

Figure 6. Comparison of simulated and experimental voltammograms obtained at a stationary glassy carbon electrode for the reduction of 50 mM ferricyanide without ASE using the indicated scan rates and R_u values.

all ionic enrichment and depletion effects are fully reproduced in the model described in the present investigation.

Results and Discussion

RDE experiments were undertaken on aqueous solutions containing 50 mM $K_3[Fe(CN)_6]$ or $K_4[Fe(CN)_6]$ in the absence or presence of 1 M KCl as the added supporting electrolyte. As noted in the Introduction, the high concentration of electroactive material was chosen to avoid complications with diffuse double layer effects. The following parameters were assumed in the simulations of voltammograms, with diffusion coefficients taken from the literature,[35] for a temperature of 298 K. The error between these values and those which might be expected at 293 K is approximately 1.7%. The ionic strength of the 50 mM solutions without supporting electrolyte was still considerable (300 mM for $K_3[Fe(CN)_6]$ or 400 mM for $K_4[Fe(CN)_6]$), and therefore even though no ASE was present, the diffusion coefficients would not be expected to differ greatly from those reported for similar total ionic strengths achieved as a combination of a lower analyte concentration with ASE. The reference cited shows a change of diffusion coefficient of less than 3% for a variation in ionic strength from 0.2 to 2 M for both $[Fe(CN)_6]^{3-}$ and $[Fe(CN)_6]^{4-}$.

For $[Fe(CN)_6]^{3-}$ $D = 7.6 \times 10^{-6}$, for $[Fe(CN)_6]^{4-}$ $D = 6.3 \times 10^{-6}$, and for both K^+ and Cl^- $D = 2 \times 10^{-5}$. For 50 mM aqueous $K_3[Fe(CN)_6]$ a kinematic viscosity, ν, of 8.82 $cm^2\ s^{-1}$ was used, and for $K_4[Fe(CN)_6]$ 8.80 $cm^2\ s^{-1}$ was used. These values were calculated assuming no volume change on addition of dissolved solid (i.e., only the density increases) and an original intrinsic viscosity η of 8.937 kg $m^{-1}\ s^{-1}$ for water, with the kinematic viscosity found as $\nu = \eta/\rho$.

For 1 M aqueous KCl containing 50 mM $K_3[Fe(CN)_6]$, ν was taken as 8.21 $cm^2\ s^{-1}$, and for 1 M aqueous KCl containing 50 mM $K_4[Fe(CN)_6]$, ν was taken as 8.20 $cm^2\ s^{-1}$. The value of $E^{o\prime}$ (formal reversible potential) was taken to be 0.183 V against Ag/AgCl, and the glassy carbon electrode area was taken to be 0.067 cm^2.

A charge-transfer coefficient α of 0.5 and heterogeneous charge-transfer rate constant k^0 of 0.04 cm s^{-1} were used for reduction of 50 mM $K_3[Fe(CN)_6]$ in the absence of ASE and in

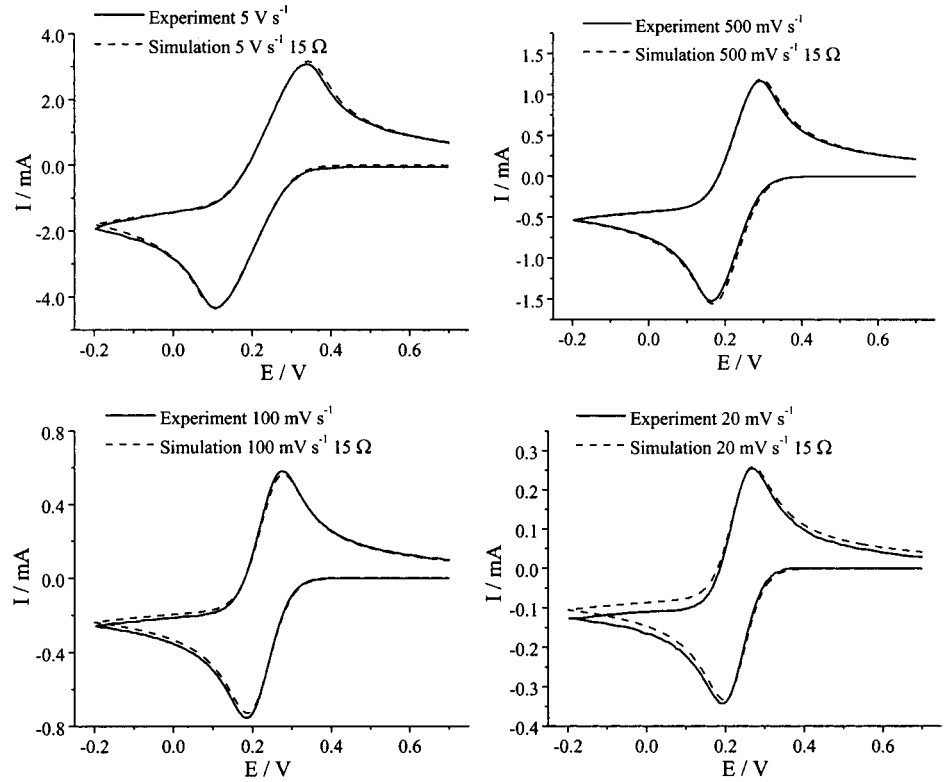

Figure 7. Comparison of simulated and experimental voltammograms obtained at a stationary glassy carbon electrode at various scan rates for the reduction of 50 mM ferricyanide in the presence of 1 M KCl as ASE, using the R_u values indicated.

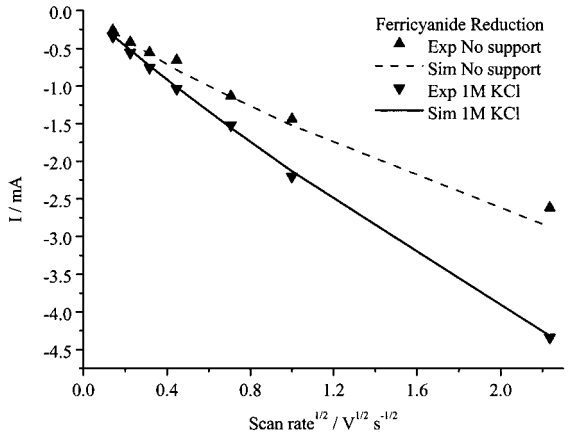

Figure 8. Comparison of simulated and experimentally determined peak currents obtained at a stationary glassy carbon electrode for the reduction of 50 mM $[Fe(CN)_6]^{3-}$ as a function of scan rate.

the presence of 1 M KCl. No attempts to provide small improvements in particular theory−experiment comparisons by varying these parameters was undertaken, as the fit in the global sense over a wide range of conditions was excellent.

Limiting Currents at a Rotating Disk Electrode. A comparison of simulated and experimental cyclic voltammograms obtained for reduction of 50 mM $K_3[Fe(CN)_6]$ at a glassy carbon RDE using a scan rate of 20 mV s^{-1} is shown in Figure 2 at rotation rates of 100 and 1000 rpm. The measured value of R_u was included in this and all other simulations, and is shown in the legend.

Agreement between theory and experiment is generally excellent. The hysteresis observed at the lower rotation rate of 100 rpm indicates that the system is not at the true steady state while traversing the escarpment region of the voltammogram. However, the limiting current is maintained for an interval of 200 mV, or 10 s, indicative that the response is very close to the true steady-state value.

An extensive series of RDE experiments at a scan rate of 20 mV s^{-1} and a range of rotation rates was performed for the reduction of ferricyanide and for the oxidation of ferrocyanide, both with and without 1 M KCl ASE. In all cases the limiting currents obtained from the rotating disk experiments agree very well with the simulations performed for both the supported and unsupported experiments, as shown in Figure 3. The Levich equation is shown to predict the limiting current well for the supported $K_4[Fe(CN)_6]$ oxidation, but less well for the supported $K_3[Fe(CN)_6]$ oxidation. This indicates that, even at a 20-fold excess of KCl ASE, the ferricyanide/ferrocyanide process is not fully supported, and that migratory effects may still play a role. The difference is presumably due to the additional K^+ concentration available with $K_4[Fe(CN)_6]$ in relation to $K_3[Fe(CN)_6]$.

The predictions of Oldham[16] for the RDE limiting currents are also shown in Figure 3, and agree very well with experiment for the ferrocyanide oxidation, and moderately well for the ferricyanide reduction. The simulation differs from Oldham's model in that the modified velocity profile given in eq 31 is used, and inhomogeneous diffusion is considered. When a simulation is undertaken using the solution velocity given by eq 2, for a test case where homogeneous diffusion prevails, the results then agree with Oldham's predictions to better than 3 significant figures.

Voltammetry at a Rotating Disk Electrode. The data in Figures 2 and 3 were obtained at slow scan rates, which led to near-steady-state conditions being achieved, as evidenced by the sigmoidal-shaped voltammograms. At scan rates sufficiently high so as to cause total concentration polarization while the diffusion layer is not fully developed, peaked cyclic voltammograms may be obtained at rotating disk electrodes, resembling those encountered at stationary electrodes. Figures 4 and 5 show

the experimental and simulated voltammograms obtained for the reduction of ferricyanide with and without ASE at various scan rates.

The simulated voltammograms are again shown to be in excellent agreement with the experimental results. The transition from a predominantly transient form at high scan rates to a steady-state form at slow scan rates as the rate of mass transport exceeds the rate of change of the concentrations at the electrode surface is evident.

Cyclic Voltammetry at a Stationary Disk Electrode. In view of the successful theory−experiment comparison achieved in the RDE experiments, the ability of the same simulation program to model transient processes was investigated using the same electrode, but in a stationary mode (zero rotation rate).

Figure 6 shows cyclic voltammograms of the unsupported reduction of 50 mM ferricyanide at scan rates between 5 V s^{-1} and 20 mV s^{-1}.

Perusal of Figure 6 shows that generally excellent agreement between theory and experiment is achieved at scan rates below 5 V s^{-1}. At higher scan rates the IR_u term becomes very large, and the differences between the staircase waveform applied and the analogue waveform assumed theoretically may also become significant. However, it is only in the region of the peaks that the results at faster scan rates (e.g., 5 V s^{-1}) become marginally less satisfactory with respect to the agreement of simulated and experimental voltammograms. Additionally the influence of natural convection can clearly be seen at the lower scan rates,[20] as the experimental current progressively exceeds that of the simulation following the peaks. Thus, it is at intermediate scan rates in the range of about 1 V s^{-1} to 100 mV s^{-1} where complete agreement between theory and experiment is observed.

Cyclic voltammograms of the supported reduction of ferricyanide at scan rates between 5 V s^{-1} and 20 mV s^{-1} are presented in Figure 7. In all cases, except at very slow scan rates of 20 mV s^{-1}, where natural convection effects are important, agreement between theory and experiment is excellent, suggesting that the problems observed at very high scan rates in the absence of ASE are associated with the large IR_u drop, and not with the staircase waveform used.

The excellent agreement of the simulated and measured peak currents for the cyclic voltammetric results obtained as a function of scan rate shown in Figure 8 confirms that cyclic voltammetry without added ASE is viable provided diffuse double layer effects can be avoided. However, the correspondence between the simulated and experimental data is less close for the unsupported reduction for the higher scan rates, as noted previously.

Conclusions

The use of macroelectrodes in voltammetric studies on solutions without ASE is accompanied by significant IR_u drop effects. However, the present study shows that if these IR_u effects are anticipated, and dealt with in a suitable simulation model, then their effects pose no significant barrier to quantitative interpretation of experimental data. The use of the RDE, even when only moderate rotation rates are employed, is shown to eliminate problems with natural convection that are enhanced in the absence of ASE.[19] The use of stationary electrodes is shown to provide qualitatively useful voltammograms at scan rates sufficiently fast to minimize natural convection. The excellent agreement with theory in the absence of ASE would be compromised when dilute double layer effects are active, as certainly would be the case in studies of the $[Fe(CN)_6]^{3-/4-}$ process at the usual millimolar concentration level.[20]

Acknowledgment. The award of an IREX Fellowship to N.P.C.S. and financial support from the Australian Research Council are gratefully acknowledged. S.W.F. gratefully acknowledges the support of the Division of Chemical Sciences, Geosciences and Biosciences, Office of Basic Energy Sciences, U.S. Department of Energy, Contract No. DE-AC02-98CH10886.

References and Notes

(1) Heyrovsky, J.; Kuta, J. *Principles of Polarography*; Academic Press: New York, 1966; see also references therein.
(2) Amatore, C.; Fosset, B.; Bartlet, J.; Deakin, M. R.; Wightman, R. M. *J. Electroanal. Chem.* **1988**, *256*, 255.
(3) Hyk, W.; Stojek, Z. *J. Electroanal. Chem.* **1997**, *422*, 179.
(4) Hyk, W.; Palys, M.; Stojek, Z. *J. Electroanal. Chem.* **1996**, *415*, 13.
(5) Baker, D. R.; Verbrugge, M. W.; Newman, J. *J. Electroanal. Chem.* **1991**, *314*, 23.
(6) Pritzker, M. D. *J. Electroanal. Chem.* **1990**, *296*, 1.
(7) Daniele, S.; Corbetta, M.; Baldo, M. A.; Bragato, C. *J. Electroanal. Chem.* **1996**, *407*, 149.
(8) Ciszkowska, M.; Stojek, Z. *J. Electroanal. Chem.* **1999**, *466*, 129.
(9) Oldham, K. B.; Feldberg, S. W. *J. Phys. Chem. B* **1999**, *103*, 1699.
(10) Bond, A. M.; Feldberg, S. W. *J. Phys. Chem. B* **1998**, *102*, 9966.
(11) Oldham, K. B. *Anal. Chem.* **1997**, *69*, 446.
(12) Oldham, K. B. *J. Electroanal. Chem.* **1992**, *337*, 91.
(13) Cooper, J. B.; Bond, A. M.; Oldham, K. B. *J. Electroanal. Chem.* **1992**, *331*, 877.
(14) Amatore, C.; Deakin, M. R.; Wightman, R. M. *J. Electroanal. Chem.* **1987**, *220*, 49.
(15) Myland, J. C.; Oldham, K. B. *Electrochem. Commun.* **1999**, *1*, 467.
(16) Oldham, K. B. *J. Phys. Chem.* **2000**, *104*, 4703.
(17) Bard, A. J.; Faulkner, L. R. *Electrochemical Methods*; Wiley: New York, 1980; p 283.
(18) Gao, X.; Lee, J.; White, H. S. *Anal. Chem.* **1995**, *67*, 1541.
(19) Bond, A. M.; Coomber, D. C.; Feldberg, S. W.; Oldham, K. B.; Vu, T. *Anal. Chem.* **2001**, *73*, 352.
(20) Rooney, M. B.; Coomber, D. C.; Bond, A. M. *Anal. Chem.* **2000**, *72*, 3486.
(21) Lee, C.; Anson, F. C. *J. Electroanal. Chem.* **1992**, *323*, 381.
(22) Norton, J. D.; White, H. S.; Feldberg, S. W. *J. Phys. Chem.* **1990**, *94*, 6772.
(23) Kissinger, P. T. In *Laboratory Techniques in Electroanalytical Chemistry*; Kissinger, P. T., Heineman, W. R., Eds.; Dekker: New York, 1984; Chapter 7.
(24) He, P.; Avery, J. P.; Faulkner, L. R. *Anal. Chem.* **1982**, *52*, 1313A.
(25) Feldberg, S. W. In *Electroanalytical Chemistry*; Bard, A. J., Ed.; Dekker: New York, 1969; Vol. 3, pp 199−296.
(26) Orlik, M. *J. Electroanal. Chem.* **1997**, *434*, 139.
(27) Milner, D. F.; Weaver, M. J. *Anal. Chim. Acta* **1987**, *198*, 245.
(28) Imbeaux, J. C.; Savéant, J. M. *J. Electroanal. Chem.* **1970**, *28*, 325.
(29) Imbeaux, J. C.; Savéant, J. M. *J. Electroanal. Chem.* **1971**, *31*, 183.
(30) Levich, V. G. *Physicochemical Hydrodynamics*; Prentice Hall: Engelwood Cliffs, NJ, 1962.
(31) Feldberg, S. W.; Bowers, M. L.; Anson, F. C. *J. Electroanal. Chem.* **1986**, *215*, 11.
(32) Bento, M. F.; Thouin, L.; Amatore, C.; Montenegro, M. I. *J. Electroanal. Chem.* **1998**, *443*, 137.
(33) Bento, M. F.; Thouin, L.; Amatore, C. *J. Electroanal. Chem.* **1998**, *446*, 91.
(34) Amatore, C.; Thouin, L.; Bento, M. F. *J. Electroanal. Chem.* **1999**, *463*, 45.
(35) Reference 1, pp 105−106.